Hindawi
Geofluids
Volume 2022, Article ID 4688347, 20 pages
https://doi.org/10.1155/2022/4688347

Research Article

Study on the Mechanism of Liquid Carbon Dioxide Fracturing and Permeability Enhancement Technology in Low Permeability Thick Coal Seam

Rui Yu,[1,2] Xinfeng Wang,[1,3] Zhaofeng Wang,[4] Long Wang,[3] Xiaoqiang Zhang,[3] Wengang Liu,[3] and Qiao Zhang[3]

[1]*School of Mines, China University of Mining and Technology, Xuzhou, Jiangsu 221116, China*
[2]*China Coal Huajin Group Co., Ltd, Hejin, Shanxi 043300, China*
[3]*School of Environment and Resources, Xiangtan University, Xiangtan, Hunan 411105, China*
[4]*College of Safety Science and Engineering, Henan Polytechnic University, Jiaozuo, Henan 411105, China*

Correspondence should be addressed to Xinfeng Wang; wangxinfeng110@126.com

Received 24 August 2022; Revised 23 September 2022; Accepted 30 September 2022; Published 14 October 2022

Academic Editor: Zhongwei Wu

For the urgent need of gas management in high gas and coal and gas herniated mines, liquid CO_2 fracturing is used to increase the permeability and promote the pumping treatment of low permeability coal seams. In this paper, we construct the coal deformation and damage model, gas diffusion and seepage model, and coal seam permeability change model; simulate and solve the plastic zone and gas pressure of coal seam after fracturing with the COMSOL Multiphysics software; and set 4 different hole spacing groups of 2 m, 3 m, 4 m, and 5 m and 3 different hole layout methods of single hole, double hole, and net hole to get the best solution for liquid CO_2 fracturing. At the same time, the specific effect of liquid CO_2 on coal seam fracturing was verified by field experiments using coal seam No. 2 of the 12316 comprehensive mining working face of Wangjialing Coal Mine as the background of the study. The numerical simulation results show that the stress concentration area around the fracturing hole appears in single-hole fracturing, and the coal seam is prone to fatigue damage in this area, but the damage range is limited, and the reduction of gas pressure after fracturing is small; the fracturing effect of double-hole and net-hole fracturing is better than that of single-hole fracturing due to the existence of sufficient critical air surface. After negative pressure extraction, the coal seam gas pressure is positively correlated with the distance from extraction hole to fracturing hole, and the best extraction effect can be seen from the field experimental results with the netted hole layout at the hole distance of 3 m. The field test results show that the pure amount of gas extraction is improved about 4 times after liquid CO_2 fracturing, which proves that liquid CO_2 fracturing has a better enhancement effect on gas management in low permeability coal seams.

1. Introduction

Gas is a natural fuel resource as a companion to coal formation and is also the main source of danger in current mine mining. With the upgrading of mining technology and the progress of production method, the underground engineering resource mining gradually expands to the deep, which leads to the increase of ground stress on coal seams and the gradual closure of fissures between coal seams, making the pressure and concentration of gas in coal seams rise, which is very easy to cause gas accidents in mines and poses a great threat to the normal mining of coal. In order to improve the permeability of deep coal seams and increase the efficiency of gas extraction, permeability-enhancing technology can be adopted to require permeability-enhancing and extraction treatment for coal seams [1–3].

Around the technical problem of liquid carbon dioxide permeability enhancement of low permeability coal seams, academics and engineers have conducted fruitful research. The liquid CO_2 fracturing technology is to inject liquid CO_2 into the coal seam, which forces the pore evolution of the coal body and the expansion and extension of the

original fractures and the generation of new fractures by the freezing effect at low temperature and the increase of the warming phase change, so as to achieve the purpose of increasing the permeability [4–7]. At the same time, CO_2, which becomes gaseous under the action of pressure injection pressure and phase change force, percolates and diffuses into the coal body, competes with CH_4 adsorbed on coal gas adsorption sites, and finally, under the action of partial pressure and concentration difference of injected CO_2, replaces and repels CH_4 gas on coal matrix gas adsorption sites, so that it transports and diffuses along the coal seam gas percolation channel to the gas extraction borehole, thus achieving the result of improving coal seam gas extraction. The result is to improve the efficiency of coal seam gas extraction [8–11]. In this process, firstly, the coal seam is deformed by the force, and the change of the plastic zone of the coal body is analyzed by the Flac software to obtain the evolution of the plastic zone of the coal seam around the fracture hole after the injection of liquid carbon dioxide, and the rule is that the radius of the plastic zone around the fracture hole increases gradually with the injection of liquid carbon dioxide [12–16]. The results show that the static fracturing process is mainly divided into four stages, microfracture generation, microdamage formation, large fracture formation, and fracture expansion and stabilization, and the generated fractures are distributed transversely, longitudinally, and multiangle with the blast hole as the center [17–21]. The permeability of the coal body is an important factor affecting the gas extraction effect in the coal seam, and the fractures generated after fracturing the coal body affect the porosity of the coal body, and the porosity and permeability of the coal body can be expressed numerically by the cubic law. COMSOL simulates the change of gas pressure and permeability in the fracturing process of coal body, and the effect of CO_2 on gas repulsion can be simulated [22–26]. In addition, the effectiveness of the practical application of liquid CO_2 fracturing is also affected by various factors, among which the arrangement of the fracturing hole has a great influence on the extraction effect after fracturing. Therefore, a combination of similar material model and numerical simulation was used to set the hole placement method as the variable and simulate the change of plastic zone of coal body and the change of gas pressure under different hole placement methods [27–32].

The comprehensive literature analysis found that the effectiveness of coal seam fracturing depends on the effective radius, and by establishing the mathematical relationship between a series of external factors such as ground stress, fracture water volume, fracture time, and effective radius, the negative impact of external environment on the fracturing effect can be greatly reduced, and the coal seam pumping effect can be improved. In this paper, we take No. 2 coal seam of 12316 comprehensive mining working face of Wangjialing Coal Mine as the engineering background and use a combination of numerical simulation and field experiment to establish a mathematical analysis model based on theoretical analysis of CO_2 fracturing mechanism, to study the evolution law of coal seam fracture expansion during fracturing, to obtain the permeability enhancement effect of liquid CO_2 fracturing, and to provide technical guidance for efficient gas extraction of low permeability thick coal seam.

2. Fracturing Mechanism of Liquid Carbon Dioxide

Liquid carbon dioxide is a low-temperature and low-viscosity fluid, and the frost heaving force generated by the instantaneous low-temperature freezing when it contacts with the coal body makes the weak surface of the coal structure contract coldly, resulting in new cracks. In addition, the liquid carbon dioxide injected into the coal seam will produce convective heat transfer with the coal body when it is seepage and diffusion in the original fracture. The liquid carbon dioxide temperature rises and phase changes, and the phase change pressure stress can give the coal fracture tension and shear failure, forcing the original fracture extension of the coal body and the generation of new fractures, expanding the fracture network area in the coal seam, and achieving the purpose of increasing permeability. The study shows that the adsorption capacity of carbon dioxide in coal matrix is stronger than that of CH_4, so carbon dioxide can replace coal seam gas well in the seepage diffusion of coal pore fracture, which provides a new way for gas predrainage before mining. 12316 working face of No. 2 coal seam in Wangjialing Coal Mine was selected as the test site. Firstly, the physical and mechanical mechanism of liquid carbon dioxide fracturing technology in coal seam permeability enhancement and drainage promotion was theoretically analyzed, and the fluid-solid coupling simulation method was used to study the range of liquid carbon dioxide fracturing and its influence on gas drainage under different hole arrangement modes. Finally, combined with the geological conditions of 12316 working face, the industrial test of gas displacement by injecting liquid carbon dioxide in coal seam was carried out to explore the technology suitable for this coal seam, put forward the key parameters for field application, and examine the gas drainage effect of the test coal seam.

In the process of injecting liquid carbon dioxide into coal seam, the coal seam is affected by three comprehensive effects of "permeability enhancement, displacement, and displacement" to improve the efficiency of gas drainage in coal seam. Liquid carbon dioxide is a kind of low temperature fluid (temperature, 56.6°C). In the process of cyclic injection, the instantaneous low temperature effect will change the temperature field of coal seam and force the coal matrix skeleton to shrink. Under the condition of sharp temperature reduction, when the shrinkage stress produced by the temperature difference on the coal body is greater than the tensile stress, the original fracture network of the weak surface of the structure is unstable. Under the action of shrinkage stress, the fracture is broken, the overall structure of the coal seam is destroyed, and the fracture network is reconstructed. There is a certain amount of free water and bound water in the pores and fissures of coal seam. Under the action of instantaneous low temperature, the volume of water in coal body expands and freezes, which produces

compressive stress on the original pores and fissures of coal body and promotes the pore reorganization and fracture extension of coal body. In addition, the liquid carbon dioxide will exchange heat with the coal body when it flows through the pore-fracture channel, and the temperature field inside the coal seam changes alternately, resulting in low-temperature freezing-melting effect and damaging the pore-fracture structure of the coal body. Specifically, during the heat exchange, the phase change of liquid carbon dioxide heating and pressurization and the expansion of coal matrix give the internal fracture network of coal to squeeze or tension stress, forcing the expansion, extension, and generation of new fractures of coal, increasing the fracture area of coal to a certain extent, and improving the permeability. 80%–90% of CH_4 in coal exists in the adsorbed state, and its dissociated CH_4 exists in the pores and fissures of coal seam. Thermodynamic theory suggests that different gas molecules have different degrees of motion under the same external conditions. The average degree of freedom equation of gas molecules is

$$\lambda = \frac{2Z}{P}\sqrt{\pi\frac{Rt}{8M}}. \quad (1)$$

In formula (1), Z is the dynamic viscosity of gas, t is temperature, r is the molar constant of gas, p is gas pressure, and m is the molar mass of gas.

Under the same temperature and pressure conditions, the dynamic viscosity of CH_4 is much larger than that of carbon dioxide, the molecular weight of CH_4 is less than that of carbon dioxide, and the degree of freedom of CH_4 is greater than that of carbon dioxide. Therefore, the random motion of CH_4 is more intense than that of carbon dioxide. Under the action of external factors, the van der Waals force between CH_4 and coal molecules is weakened, and it is easy to desorb. A large number of studies have shown that under the same conditions, the adsorption capacity of carbon dioxide in coal matrix is stronger than that of CH_4. When the amount of carbon dioxide entering the coal CH_4 occurrence area increases, the two will produce competitive adsorption. This conclusion shows that the carbon dioxide partial pressure entering the adsorption site of coal matrix increases and the CH_4 partial pressure decreases under the action of transportation power and liquid carbon dioxide phase transition stress. The adsorption-desorption equilibrium of gas components in coal matrix is destroyed, and the carbon dioxide molecules with stronger adsorption capacity occupy the adsorption site of CH_4, so that CH_4 molecules are desorbed and replaced. With the increase of carbon dioxide injection, the concentration difference of mixed gas components at both ends of the gas migration channel is produced, and CH_4 molecule is displaced to the corresponding gas migration channel. Finally, under the dual action of pressure difference and concentration difference, a large number of CH_4 molecules flow along the coal fracture channel and diffuse to the drainage borehole. The displacement process is shown in Figure 1.

3. Mathematical Model of Crack Propagation

There are a large number of primary fractures in the coal rock, and the internal fractures are crisscross, the coal rock show typical anisotropy. The viscosity, density, permeability coefficient, and other physical parameters of various types of fracturing fluids, such as water and liquid carbon dioxide, will change over time during the increase of drilling pressure. Complexity of primary fractures in coal rock is closely related to complex variation of physical parameters of fracturing fluid. In order to deduce the fracture propagation process of liquid carbon dioxide fracturing, it is necessary to simplify the coal-rock mass and fracturing fluid.

The fracture shape of the fracturing process is simplified as shown in Figure 2. In the calculation process, due to the large buried depth of the coal seam, the direction of the major principal stress in the formation is perpendicular to the surface, and the minor principal stress is horizontal, the borehole wall of the coal seam produces cracks parallel to the axial direction of the borehole, and the relationship between injection pressure difference and crack propagation distance is established by calculation. With the increase of injection pressure difference, the fracture propagation radius increases gradually. When the injection pressure is small, the crack propagation radius is not sensitive to the change of injection pressure difference; when the injection pressure difference is large, the injection pressure has a great influence on the fracture diffusion radius, and the increase of the injection pressure will lead to the obvious change of the fracture diffusion radius.

4. Simulation of Permeability Enhancement Effect of Liquid Carbon Dioxide Fracturing

4.1. Basic Assumptions of the Model. According to the geological and gas occurrence conditions of No. 2 coal seam in 12316 fully mechanized working face of Wangjialing Coal Mine, the fluid-solid coupling model of borehole failure and gas flow in coal seam under static fracturing was established by using the COMSOL Multiphysics simulation software. The distribution characteristics of stress and plastic zone around the borehole were compared and analyzed under single-hole fracturing, double-hole fracturing, and mesh distribution control fracturing. The gas pressure relief range of the inspection hole under different extraction time was simulated, and the reasonable carbon dioxide fracturing hole distribution and extraction time were obtained.

Since the flow of gas in coal seam is affected by many factors, it is a relatively complex process. In order to make the modeling convenient and feasible, the following assumptions are made:

(1) The coal seam is mainly composed of coal matrix, matrix pores, and cracks, and the composition of pores and cracks in the coal seam is continuous

(2) Coal is heterogeneous and isotropic elastic-plastic medium, ignoring the influence of anisotropy of coal seam on permeability directivity

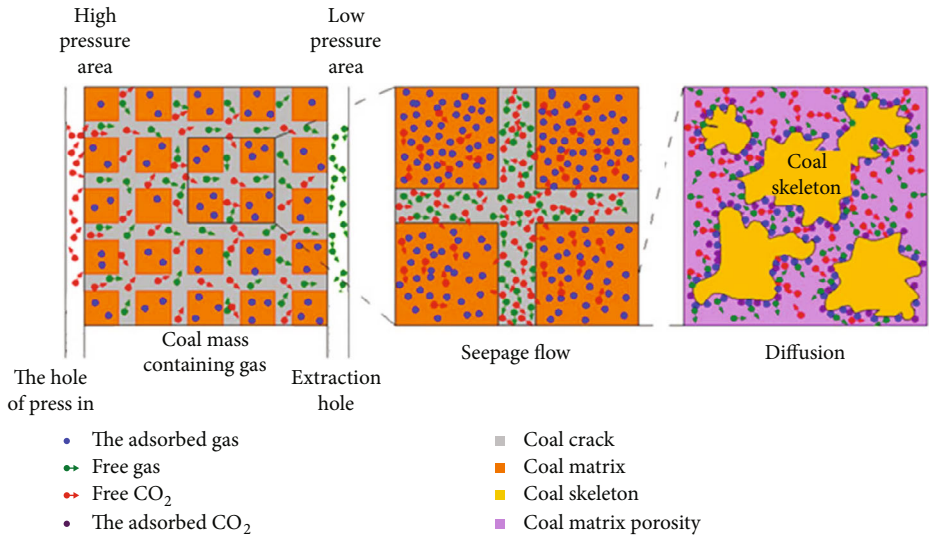

Figure 1: Chart of CH_4 in carbon dioxide displacing coal seam.

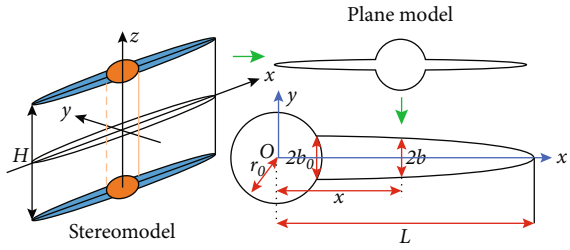

Figure 2: Diagram of crack shape.

(3) In the whole process of flow displacement, coal seam contains only carbon dioxide and gas, without considering the existence and influence of water and other gases

(4) The migration form of body in coal cracks is only seepage process, and the seepage process meets Darcy's law. The gas migration form in the coal fracture is only the diffusion process, and the diffusion process follows the Fick's law

(5) Coal failure satisfies Mohr-Coulomb criterion

4.2. Model Parameters and Boundary Conditions

4.2.1. Establishment of Geometric Model. The actual process of carbon dioxide flow displacing gas is in three-dimensional space. In order to facilitate modeling and calculation, we simplify it into two-dimensional model, ignoring the thickness of coal seam. The two-dimensional plane model established in this simulation is 12 m long and 8 m wide, and liquid carbon dioxide is injected from fracturing borehole. Because the instantaneous fracturing process of liquid carbon dioxide injected into coal seam is unpredictable, the simulation does not consider the fracture process of fracturing, only simulates the gas pressure change after precracking and the process of carbon dioxide flowing in coal seam and displacing gas. The average buried depth of the working face is 400 m, the average thickness of the coal seam is 6 m, the thickness of the roof rock is 2 m, and the thickness of the floor rock is 1.3 m. The expansion force acting on the borehole wall during the liquid carbon dioxide fracturing is approximately 10 MPa. According to the measurement results of gas content in working face, the corresponding gas pressure is 0.2 MPa according to the indirect calculation equation of Langmuir equation. Therefore, the surrounding of the model is assumed to be zero flow boundary, the roof and floor of the coal seam are impervious strata, and the rolling boundary is set around. The bottom of the model is fixed constraint, and the side of the model is horizontal constraint. The top of the model is free boundary, and the drilling boundary is free boundary. On the free boundary of the top of the model, a 10 MPa vertical downward stress is set up to express the load of the rock layer, and the load of 10 MPa is applied to the borehole wall of the model to express the force generated by liquid carbon dioxide fracturing. The initial velocity field and displacement field of the model are 0, the coal seam gas pressure is set to 0.2 MPa, the extraction negative pressure is 20 kPa, and the borehole diameter is 75 mm. Liquid carbon dioxide pumping model is shown in Figure 3.

According to the measured gas parameters, coal rock mechanical parameters, and other physical parameters of the same coal seam in coal mines and mining areas, the model parameters are determined as shown in Table 1. According to the measurement results of gas content in working face, the original gas content is 3.3 m^3/t, and the corresponding gas pressure is 0.2 MPa according to the indirect calculation equation of gas content in coal seam.

4.2.2. Setting Boundary and Initial Conditions for Numerical Simulation. For differential equations, it is necessary to point out the definite solution conditions; the most common is to determine the definite solution according to the boundary conditions and initial conditions. The boundary conditions

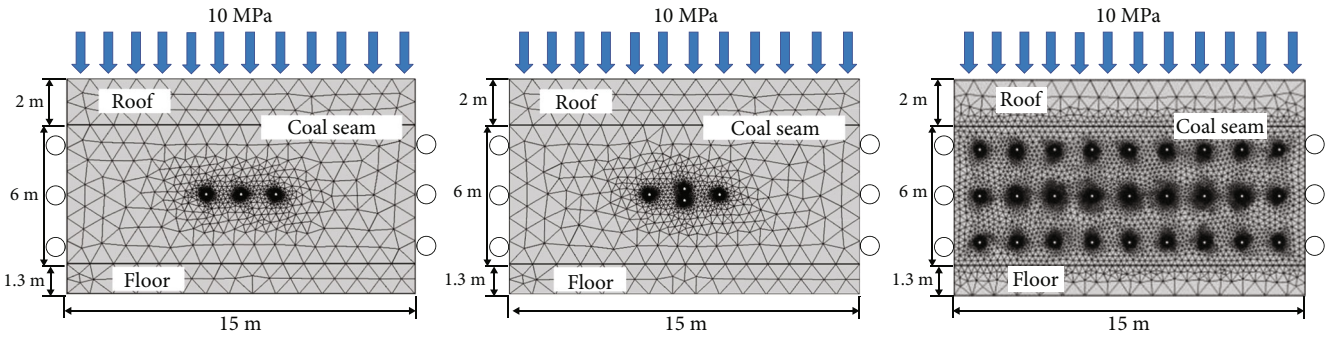

Figure 3: Geometric model of liquid carbon dioxide fracturing pumping.

Table 1: Basic parameters of liquid carbon dioxide fracturing model for No. 2 coal seam.

Physical parameter	Units	Value
Adsorption constant a	m^3/t	29.24
Adsorption constant b	MPa^{-1}	0.95
Drainage negative pressure	kPa	20
Coal seam gas pressure	MPa	0.2
Coal seam gas pressure	MPa	0.2
Klinkenberg coefficient	MPa	0.35
Coal seam cohesion	MPa	1.5
Atmosphere	MPa	0.101325
Roof cohesion	MPa	3.5
Floor cohesion	MPa	4.8
Roof elastic modulus	GPa	5.0
Elastic modulus of base plate	GPa	6.5
Elastic modulus of coal seam	GPa	3.0
Water proportion	%	0.44
Dust proportion	%	8.07
Volatile proportion	%	17.38
Porosity	%	4.3
Maximum adsorption volume expansion	%	3
Coal density	kg/m^3	1400
Density of floor	kg/m^3	2600
Roof density	kg/m^3	2300
Internal friction angle of floor	/°	37
Roof internal friction angle	/°	32
Internal friction angle of coal	/°	25
Gas universality coefficient	J/(mol·K)	8.314
Initial permeability of coal seam	m^2	$0.2 \times e - 14$
Poisson's ratio of coal seam	—	0.35
Dynamic viscosity	Pa·s	$1.08 \times e - 5$

of flow field generally include pressure boundary conditions and flow boundary conditions, namely,

$$p = p(t). \tag{2}$$

In formula (2), $p(t)$ is the pressure given on the boundary.

The initial condition is the value of the unknown function and its partial derivatives to time at the initial time $t = 0$. The initial condition for the flow field is the fluid pressure distribution in the solution domain, which is

$$p = p(x, y, z). \tag{3}$$

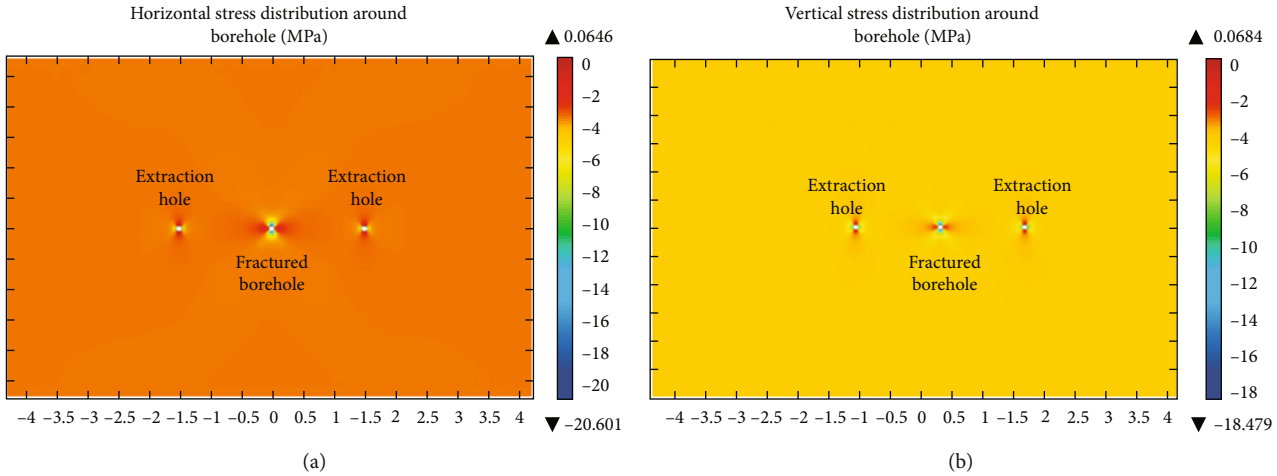

Figure 4: Stress distribution around borehole after liquid carbon dioxide fracturing.

5. Simulation Result Analysis

5.1. Simulation Analysis of Single-Hole Fracturing Effect. In the model, the roadway is the atmospheric pressure constant pressure boundary, and the extraction borehole is the extraction negative pressure constant pressure boundary. The size of the single-hole liquid carbon dioxide fracturing model is 15 m × 9.3 m (the thickness of coal seam is 6 m, the thickness of roof rock is 2 m, and the thickness of floor is 1.3 m). The model is assumed to be zero flow boundary around the model, and the support is set around the left and right. The fixed constraint is set at the bottom of the model, and the horizontal constraint is set at the side of the model. The vertical stress of 10 MPa is set at the top of the model according to the field test data, and three boreholes with 75 mm diameter are excavated in the middle of the model (liquid carbon dioxide fracturing agent is injected into the middle borehole as the fracturing hole, and the two boreholes are the extraction inspection hole, and the interval between the fracturing hole and the extraction hole is 1.5 m). The negative pressure of the extraction hole is 20 kPa. When the fracturing pressure is 10 MPa, the stress distribution around the borehole is shown in Figure 4.

As can be seen from Figure 4(a), the pressure relief range of the borehole is also small due to the small aperture of the extraction borehole ($\phi = 75$ mm); with the increase of the expansion load on the wall of the fracturing hole, the influence area of the horizontal stress around the fracturing hole is obviously larger than that of the extraction hole, and the obvious stress concentration appears on both sides of the fracturing hole (the peak stress reaches 9.6 MPa) and gradually transfers to the deep coal seam, and the stress reduction zone appears on the upper and lower sides of the fracturing hole. As shown in Figure 4(b), the vertical stress concentration appears in the upper and lower sides of the fracturing hole, and the stress influence range of the fracturing hole is significantly larger than that of the drainage inspection hole. The pressure relief zone appears on the left and right sides of the fracturing hole, which is due to the fact that in the process of liquid carbon dioxide fracturing, after the initiation pressure in the fracturing hole exceeds the ultimate tensile strength of the coal around the hole, the coal around the hole begins to break and produces a large number of cracks to relieve pressure.

In order to further explore the damage and cracking around the borehole after liquid carbon dioxide fracturing, the distribution map of the plastic zone around the borehole is derived, as shown in Figure 5. For coal, the yield of elastic-plastic material is failure; that is, the area where plastic strain occurs is the area where coal is damaged.

It can be seen from Figure 5 that the distribution of plastic zone around the fracturing hole is significantly larger than that of the pumping hole. The plastic zone of the fracturing hole presents a spindle-shaped distribution. The plastic zone extends about 0.12 m horizontally to the left and right sides, 0.522 m vertically upward, and 0.477 m downward. The plastic zone of the extraction hole is butterfly wing distribution, and the radius of the plastic zone is about 0.11 m. This shows that the obvious plastic deformation of coal around the fracturing hole occurs after the crack initiation pressure is applied to the fracturing hole wall, which also greatly promotes the development of coal seam cracks, resulting in a significant increase in the permeability of coal in the region.

In order to investigate the effect of liquid carbon dioxide fracturing on gas drainage, it is necessary to compare and analyze the gas pressure relief range of the inspection hole under different extraction time. When the drainage time is 10 d, 30 d, 90 d, and 180 d, the gas distribution around the borehole is shown in Figure 6.

In Figure 6, the vertical and horizontal coordinates are position size, and the right graphic unit is gas pressure. It can be seen from Figure 6 that with the increase of extraction time, the gas content around the extraction borehole on both sides of the fracturing hole decreases continuously, and the influence range of extraction pressure relief is expanding. The variation range of gas pressure around the drainage borehole is obviously larger than that in the far area. In the initial pumping, the gas pressure gradually increases with the increase of time, and the pressure drop coefficient is large.

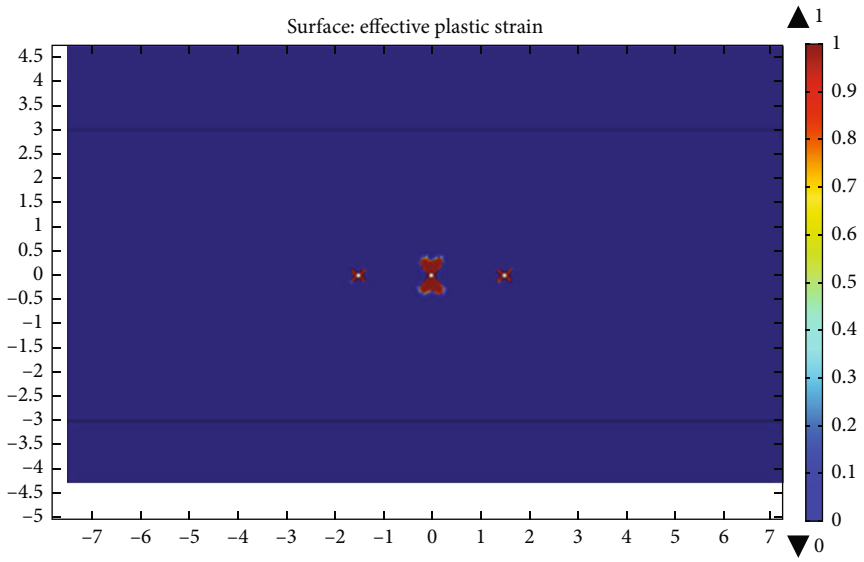

Figure 5: Plastic zone distribution of single-hole fracturing.

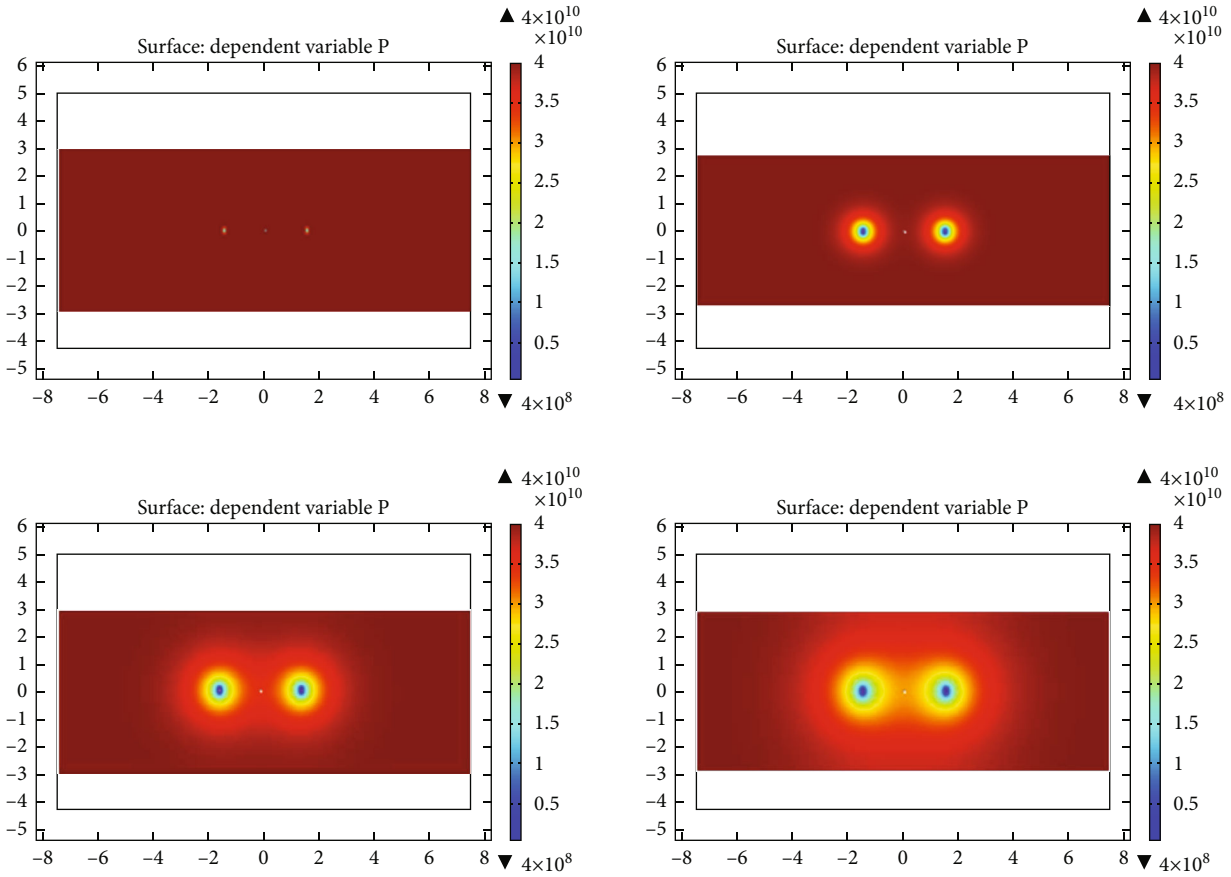

Figure 6: Gas pressure distribution chart of single-hole fracturing.

However, with the continuous growth of time, the downward trend of pressure gradually becomes smaller, and the reduction rate gradually becomes smaller and tends to ease.

The cloud picture of gas pressure distribution at 180 d of extraction was amplified, and the left extraction hole was taken as the observation point, as shown in Figure 7.

It can be seen from Figure 7 that after 180 days, the gas pressure drops to 0.120 MPa at 0.20 m from the extraction hole. At 1.49 m from the extraction hole, the gas pressure decreased to 0.184 MPa. The closer the extraction hole is to the side of the fracturing hole, the more obvious the pressure relief of gas pressure is. The gas pressure around the

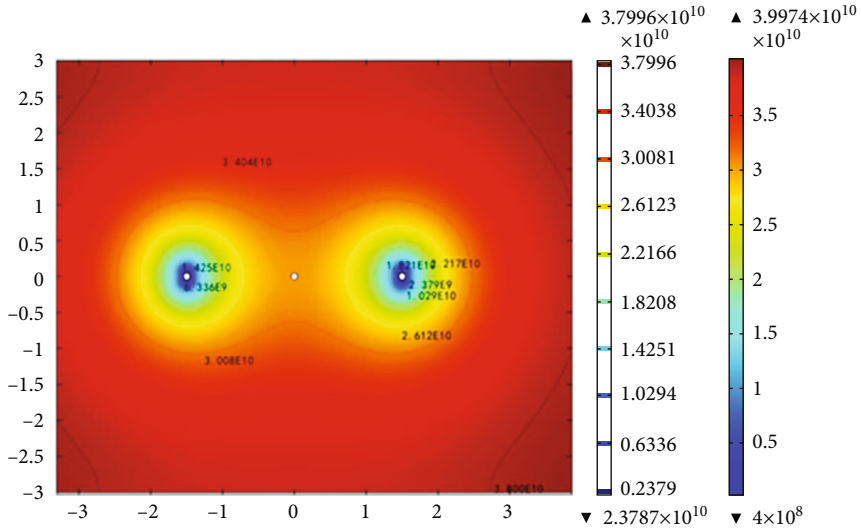

Figure 7: Gas pressure distribution around borehole after 180 days.

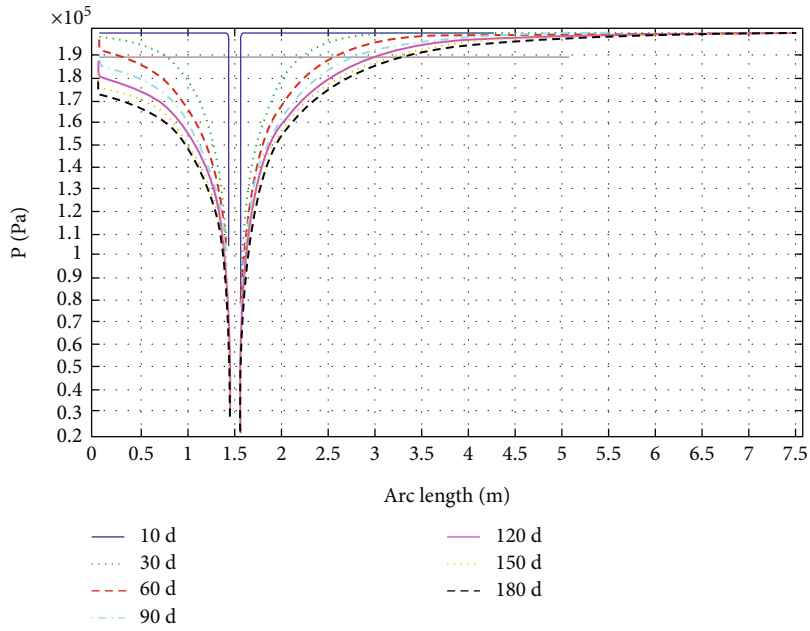

Figure 8: Gas pressure relief curve of single-hole fracturing drilling.

extraction hole shows an asymmetric distribution, indicating that the permeability of coal near the side of the fracturing hole is high.

According to the actual production requirements, this extraction standard is based on the extraction rate of the coal seam reaching 20%, and the distance from the borehole center to the gas pressure drop of 0.189 MPa is the effective extraction range of gas. The gas pressure relief curve under different extraction time is shown in Figure 8.

It can be seen from Figure 8 that when the liquid carbon dioxide fracturing is carried out in a single borehole, the gas pressure of the drainage borehole decreases to 0.189 MPa at 10 d, 30 d, 60 d, 90 d, 120 d, 150 d, and 180 d, and the unilateral gas pressure relief ranges are 0.07 m, 0.70 m, 1.06 m, 1.29 m, 1.46 m, 1.55 m, and 1.79 m, respectively. The pressure relief range at 180 d is 38.75% higher than that at 90 d, and the pressure relief range at 90 d is 84.85% higher than that after 30 d. The data show that after liquid carbon dioxide fracturing, the gas pressure relief range around the borehole gradually increases with the increase of extraction time, but after 90 d, the growth rate of pressure relief range gradually decreases with the extension of extraction time.

5.2. Simulation Analysis of Double-Hole Fracturing Effect. Double-hole fracturing effect is mainly affected by ground stress, drilling along the direction of maximum principal stress or perpendicular to the direction of minimum principal stress. In order to solve the problem of insufficient coal

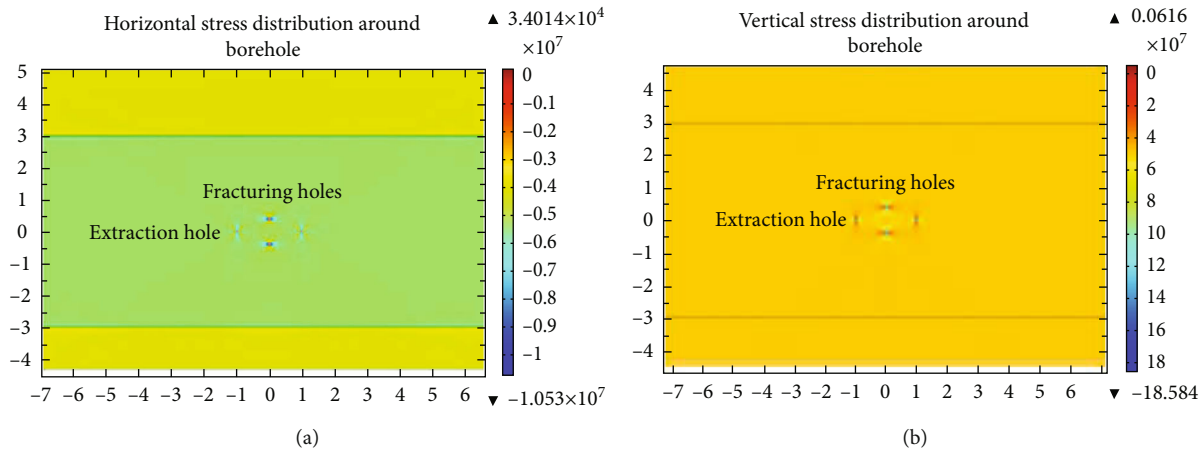

Figure 9: Stress distribution map of two-hole fracturing with 2 m spacing between pumping holes.

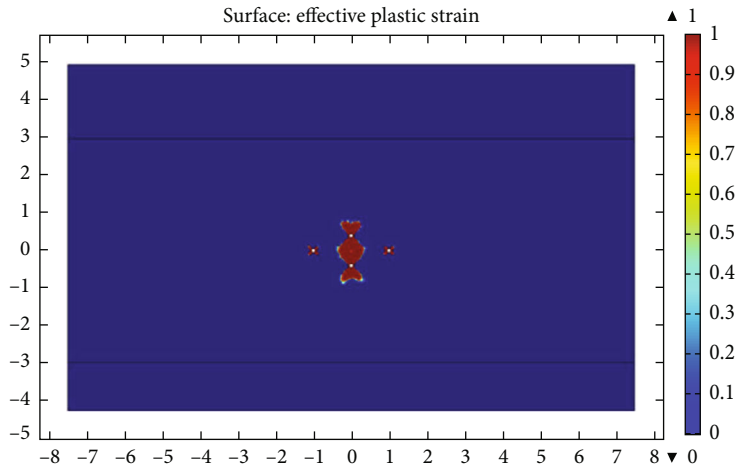

Figure 10: Distribution of plastic zone around double-hole fracturing borehole.

seam face, two fracturing holes can be arranged up and down at the same position to realize the coupling effect of in situ stress and stress disturbance between fracturing boreholes, which is equivalent to the torque synthesis theorem, so that the borehole extends along its resultant force direction (when the hole distance is large, it is equivalent to two single-hole splitting). The fracturing failure process can be divided into three stages: stress accumulation, crack stable propagation, and instability failure. The maximum principal stress at the observation point between two holes will correspond to the stress drop zone and the energy accumulation zone with the increase of calculation steps. The change of initial fracture pressure is not obvious when the borehole spacing is small, while the initial fracture pressure increases with the increase of lateral pressure coefficient when the borehole spacing is large. The dual-hole liquid carbon dioxide fracturing is carried out, and the size of the dual-hole fracturing model is 15 m × 9.3 m. The zero flow boundary is assumed around the model, and the rolling boundary is set around the left and right. The bottom of the model is fixed constraint, the side of the model is horizontal constraint, and the top of the model is applied with 10 MPa vertical stress. Two fracturing holes with a diameter of 75 mm were arranged up and down in the middle of the model, and the spacing was 0.5 m. During the fracturing of liquid carbon dioxide, 10 MPa initiation pressure was applied on the hole wall. In order to investigate the influence range of dual-hole fracturing, the drainage inspection holes are arranged on the left and right sides of the fracturing hole, and the spacings of the two drainage holes are 2 m, 3 m, 4 m, and 5 m, respectively. The permeability enhancement effect of dual-hole fracturing is analyzed as follows.

When the distance between the two extraction holes is 2 m, the stress distribution around the borehole after the liquid carbon dioxide fracturing of the two holes is shown in Figure 9.

It can be seen from Figure 9(a) that in the dual-hole fracturing, the horizontal stress relief range at the upper and lower ends of the fracturing hole further increases due to the two fracturing holes acting as free surfaces, and they begin to overlap with each other. The horizontal stress concentration on the left and right sides of the fracturing hole is also gradually transferred to the deep part of the coal seam, which is larger than that of the single-hole fracturing. As

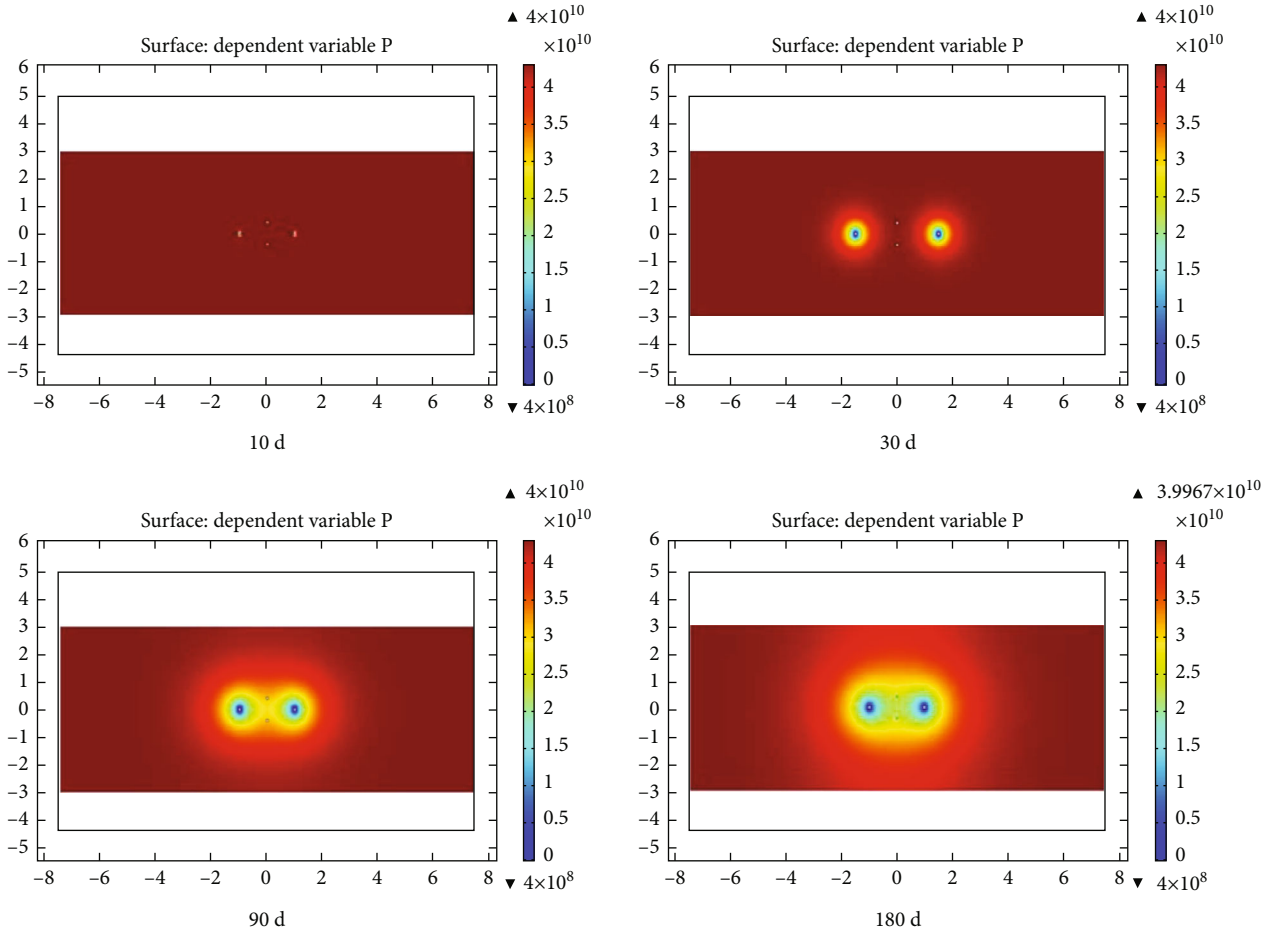

Figure 11: Gas pressure distribution map of two-hole liquid carbon dioxide fracturing with interval of 2 m.

shown in Figure 9(b), the influence range of vertical stress of double-hole fracturing is larger than that of single-hole fracturing, and the pressure relief area near the side of the fracturing hole is almost quickly opened, which shows that in the process of double-hole fracturing, the coal around the upper and lower two boreholes produces greater fracture pressure relief.

The distribution of plastic zone around the borehole after two-hole liquid carbon dioxide fracturing is up and down fishtail, and the plastic stress extends horizontally, as shown in Figure 10.

As shown in Figure 10, it can be seen that the plastic failure zones around the upper and lower fracturing holes are interconnected during the double-hole fracturing. The plastic zone extends about 0.365 m horizontally on both sides, 0.818 m vertically upward, and 0.840 m downward. Compared with single-hole fracturing, the failure range of plastic zone further increases.

The gas distribution around the borehole of double-hole fracturing at the interval of 2 m is shown in Figure 11.

It can be seen from Figure 11 that with the increase of extraction time, the gas pressure around the extraction boreholes on both sides of the fracturing hole decreases continuously, and the range of extraction and pressure relief gradually expands and begins to be opened. The pressure relief effect of double-hole fracturing is significantly greater than that of single-hole fracturing. In the early stage of extraction, the pressure relief area of the two extraction holes was circular and gradually evolved into "∞" distribution after 30 days. The pressure relief effect near the side of the fracturing hole was more obvious.

When the spacing between the two pumping holes is 3 m, the gas distribution around the borehole after the liquid carbon dioxide fracturing of the two holes is shown in Figure 12.

It can be seen from Figure 12 that as the extraction time increases, the gas pressure around the extraction boreholes on both sides of the fracturing hole decreases continuously, and the pressure relief effect of double-hole fracturing is still significantly greater than that of single-hole fracturing. However, after 30 days of extraction, due to the increase in the spacing between the two drainage holes, the gas pressure relief range is not connected. After 90 days, the pressure relief area gradually evolves into a "∞" distribution and begins to be connected. The pressure relief effect near the side of the fracturing hole is more obvious.

When the distance between the two pumping holes is 4 m, the gas distribution around the borehole after the liquid carbon dioxide fracturing of the two holes is shown in Figure 13.

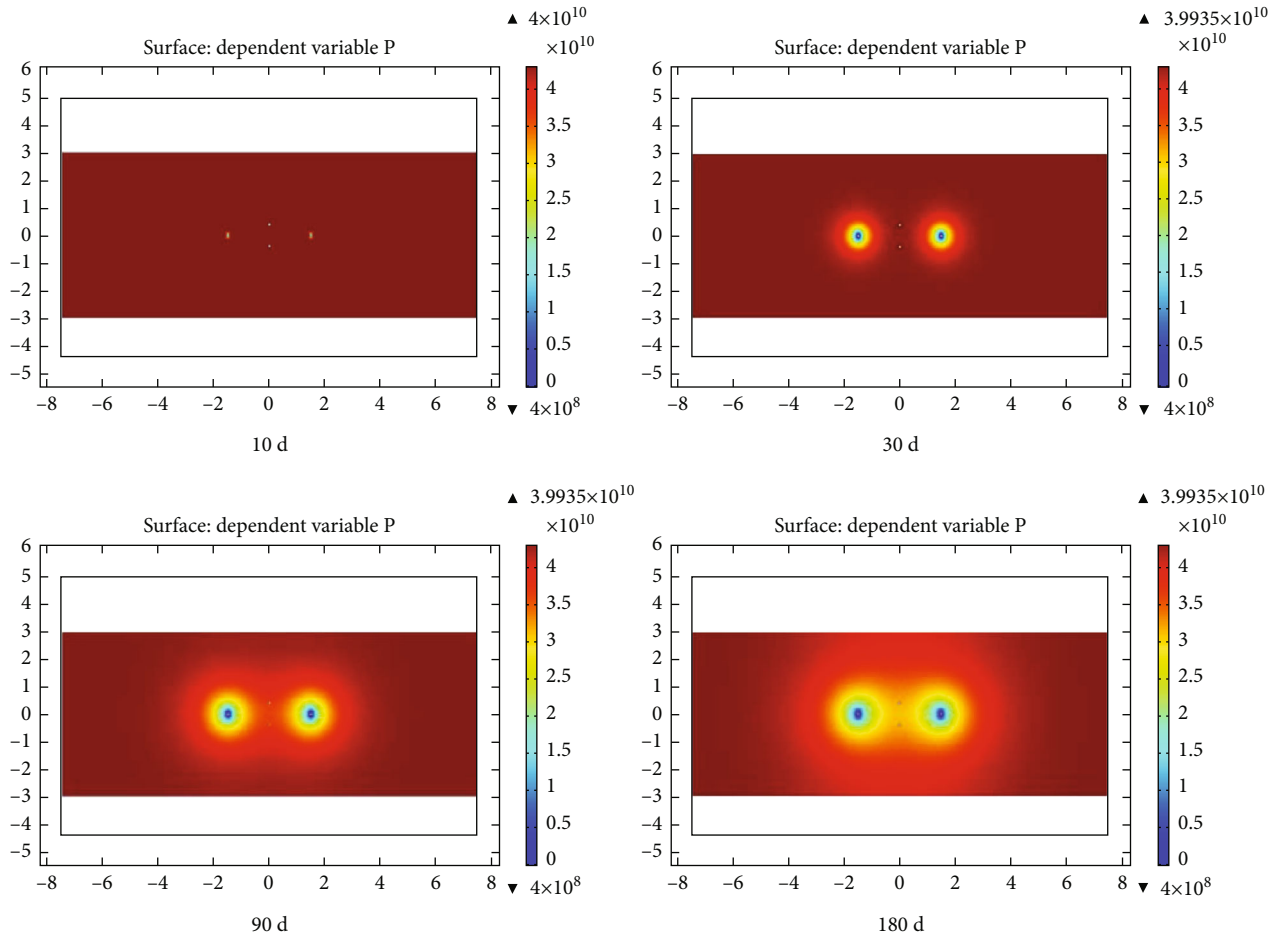

Figure 12: Gas pressure distribution map of liquid carbon dioxide fracturing with 3 m spacing between pumping holes.

It can be seen from Figure 13 that with the further increase of the spacing between the two extraction holes, the pressure relief range of the gas after 90 days of extraction is not fully conduction, but the pressure relief effect of the extraction hole near the side of the fracturing hole is still obvious.

When the distance between the two pumping holes is 5 m, the gas distribution around the borehole after the liquid carbon dioxide fracturing of the two holes is shown as Figure 14.

It can be seen from Figure 14 that with the further increase of the spacing between the two drainage holes, the gas pressure relief range after 90 d of extraction is not connected. After 180 d, the pressure relief area gradually evolves into a "∞" shape distribution and begins to be connected, but the pressure relief effect of the drainage hole near the side of the fracturing hole is still obvious.

In order to compare the pressure relief effect of two-hole liquid carbon dioxide fracturing with four different spacing extraction holes, the relationship between the range of pressure relief zone on one side of the extraction hole and the extraction time is drawn as shown in Figure 15.

It can be seen from Figure 15 that in the same extraction cycle, the smaller the distance between the extraction hole and the fracturing hole is, the larger the range of gas pressure relief is. Within 10 d-90 d of extraction, the gas pressure relief effect of dual-hole fracturing is the most obvious, and then, the radius of gas pressure relief area increases slowly with time and tends to be stable after 180 d. When the spacing between the two extraction holes is set to 3 m, good gas extraction effect can be achieved.

When the drainage hole spacing is 3 m, the gas pressure relief effect of double-hole liquid carbon dioxide fracturing in the same drainage period is obviously better than that of single-hole fracturing. When the extraction time was 30 d, the unilateral pressure relief range of double-hole fracturing increased from 0.64 m to 1.40 m, an increase of 119% compared with that of single-hole fracturing. When the extraction time was 90 d, the pressure relief range of double-hole fracturing increased from 1.29 m to 2.24 m, an increase of 73.6% compared with that of single-hole fracturing. When the extraction time was 180 d, the pressure relief range of double-hole fracturing increased from 1.82 m to 2.88 m compared with that of single-hole fracturing, with an increase of 58.2%.

5.3. Simulation Analysis on Fracturing Effect of Mesh Holes. It can be seen from single-hole simulation and double-hole results that double-hole fracturing can effectively enhance the fracturing effect of liquid carbon dioxide fracturing.

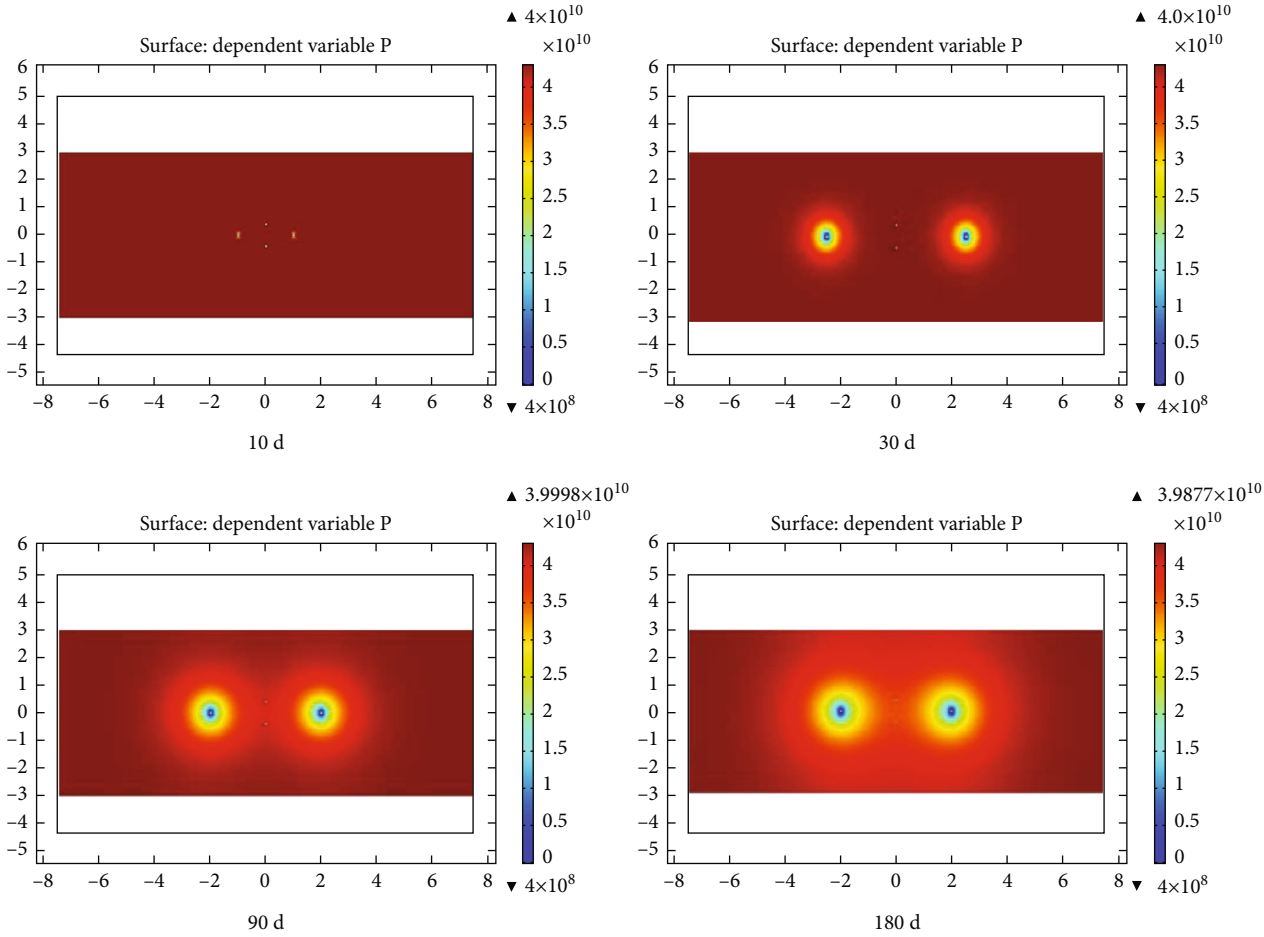

Figure 13: Gas pressure distribution map of liquid carbon dioxide fracturing with 4 m spacing between pumping holes.

The double-hole fracturing mainly relies on the stress superposition between the two holes, and the fracture of the guiding hole mainly relies on the free surface formed by the guiding hole. Therefore, on the basis of the double-hole fracturing, the grid-like distributed control liquid carbon dioxide fracturing scheme is proposed; that is, the fracturing and fracture of the double-hole + guiding hole are combined in the liquid carbon dioxide fracturing, so that the fracturing initiation pressure of the liquid carbon dioxide fracturing is superimposed, and the crisscross fracture network is formed, so as to achieve better coal seam permeability enhancement effect.

The size of mesh hole fracturing model is also 15 m × 9.3 m. The model is assumed to be zero flow boundary around, and the roller boundary is set around. The bottom of the model is fixed constraint, and the side of the model is horizontal constraint. The vertical stress of 10 MPa is applied on the top of the model. In the middle distance of No. 2 coal seam, 9 rows of drilling fields are arranged, 3 boreholes per row, the spacing of boreholes is 1.5 m, the aperture is 75 mm, the fracturing hole and the extraction hole (guide hole) are cross arranged, and the radial expansion force of 10 MPa is applied on the wall of the fracturing hole. The stress distribution around the borehole after liquid carbon dioxide fracturing is shown in Figure 16.

It can be seen from Figure 16 that there are four pumping holes around each fracturing hole as a free surface, and the free surface is greatly increased. Therefore, the horizontal stress relief range of the upper and lower ends of the fracturing hole is further increased, and the mutual conduction occurs. Compared with single-hole fracturing and double-hole fracturing, the stress influence range is significantly larger.

The distribution of plastic zone around the borehole after grid-like liquid carbon dioxide fracturing is shown in Figure 17.

As shown in Figure 17, it can be seen that after the implementation of grid-like liquid carbon dioxide fracturing in thick coal seam, the plastic failure zone around the borehole is basically interconnected, and the in situ stress in most areas of the coal seam is released, and the permeability of the coal seam is further increased.

Under different extraction time, the gas distribution around the borehole after grid fracturing is shown in Figure 18.

It can be seen from Figure 18 that after the implementation of liquid fracturing with mesh hole arrangement, the gas pressure relief effect around the drainage borehole is not obvious at 10 d of drainage. With the increase of drainage time for 30 d, the gas pressure around the drainage borehole

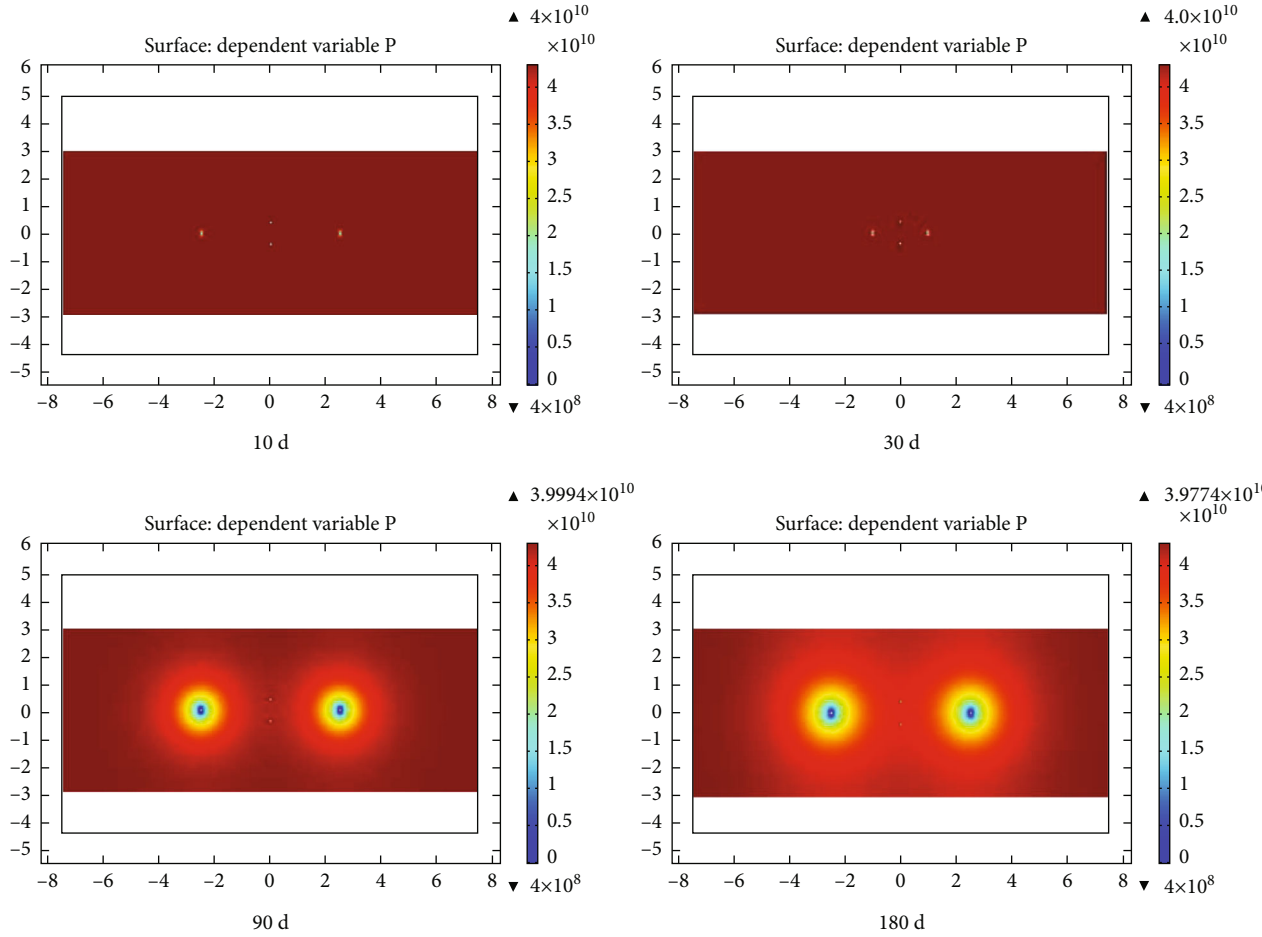

Figure 14: Gas pressure distribution map of liquid carbon dioxide fracturing with 5 m spacing between pumping holes.

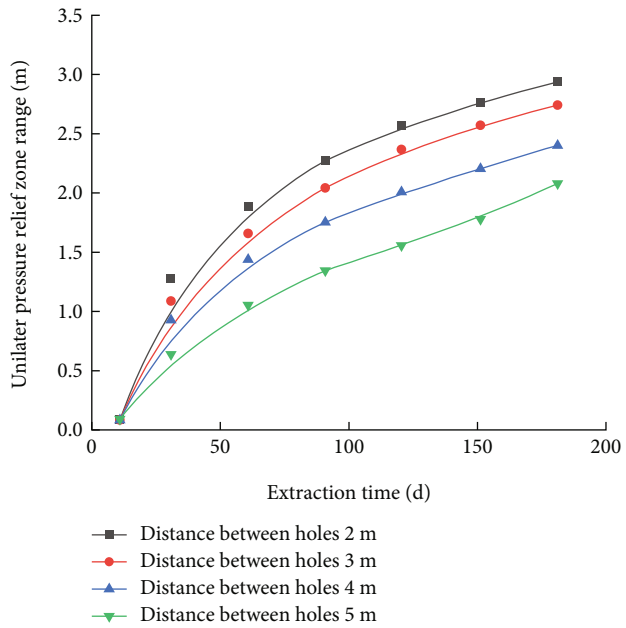

Figure 15: Relationship between pressure relief range and time under different hole arrangement in double-hole fracturing.

around the fracturing borehole is significantly reduced, and the pressure relief range is gradually expanded, and the influence of the surrounding drainage borehole has a trend of gradual penetration. After 90 days, the pressure relief area around the extraction hole has been opened and gradually expanded; after 180 days, the gas pressure of the whole coal seam was completely released.

The relationship between the gas pressure around the drainage hole and the distance in different time periods is shown in Figure 19.

It can be seen from Figure 19 that after 60 days of extraction, the gas pressure around the extraction hole is reduced to below 0.18 MPa.

Liquid carbon dioxide fracturing is accompanied by the process of carbon dioxide replacing gas in coal seam. When the air contacts with the coal surface, due to the fracture of the coal matrix and the difference of the force between the pore surface molecule and the internal molecule, there is a residual surface force field, which forms the surface potential energy. Due to the existence of the surface potential energy, the gas concentration on the pore and fracture surface of the coal body increases, and the adsorption phenomenon occurs. With the occurrence of the adsorption phenomenon, the adsorption process is accompanied by the release of the adsorption

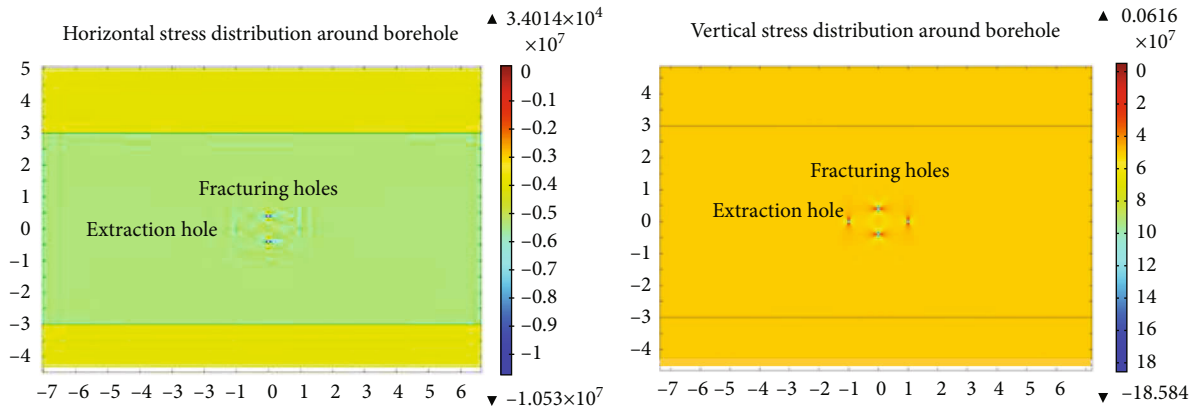

Figure 16: The stress distribution around the boreholes of mesh hole fracturing.

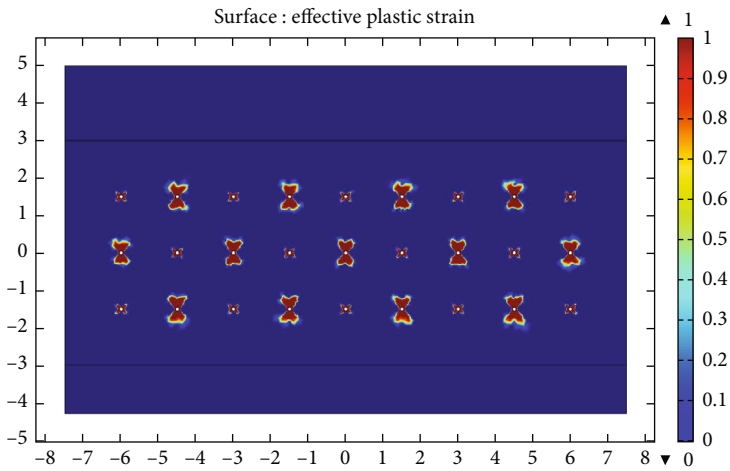

Figure 17: Distribution of plastic zone in boreholes after fracturing with mesh holes.

heat. Gas adsorption is mainly adsorbed on the surface of coal matrix, and the coal matrix has a large specific surface area, so it has strong adsorption. At the same time, the coal reservoir mainly adsorbs gas by physical adsorption, and the coalbed methane in the coal reservoir mainly exists in the adsorption state. Only when the gas molecule obtains sufficient kinetic energy and can overcome the gravitational barrier of the coal surface, the gas can be desorbed from the coal surface. Therefore, when carbon dioxide replaces gas, because the attraction of coal to carbon dioxide is much stronger than that of gas, carbon dioxide preferentially adsorbs, which reduces the adsorption force of coal to gas. When the adsorption force cannot bind gas, gas begins to change from adsorption state to free state. The displacement effect is shown in Figure 20.

Figure 20 is the distribution map of coal seam pressure in carbon dioxide displacement process under the pressure of 10 MPa, 1 h, 2 h, and 4 h. It is found that the influence range of carbon dioxide near the extraction hole is 0.76 m after 1 h, 0.98 m after 2 h, and 1.33 m after 4 h.

6. Field Experiment of Liquid Carbon Dioxide Fracturing

6.1. Introduction of Test Site. This liquid carbon dioxide fracturing experiment was selected at 60 m in front of 850 chamber of return airway of 12316 fully mechanized working face in Wangjialing Coal Mine. The roadway elevation is +500 m ~ +540 m, buried depth is about 470 m, vertical stress is $\sigma v = 11.8$ MPa, Poisson's ratio is $\upsilon = 0.335$, and the horizontal stress is $\sigma_h = v/(1-v) \bullet \sigma_v = 0.504 \times 11.8 = 5.95$ MPa. The tensile strength of coal is 0.5 ~ 1.5 MPa.

6.2. Introduction of Experimental Equipment. In order to select the technical equipment suitable for high stress and low permeability coal seam fracturing low permeability coal seam in Wangjialing Coal Mine, the carbon dioxide fracturing and permeability enhancement technical equipment system is developed by Jiangsu Tuochuang Scientific Research Instrument Co., Ltd. The equipment is shown in Figure 21.

Figure 21 is the underground high pressure liquid carbon dioxide fracturing antireflection system. The system mainly includes liquid carbon dioxide pressurization system,

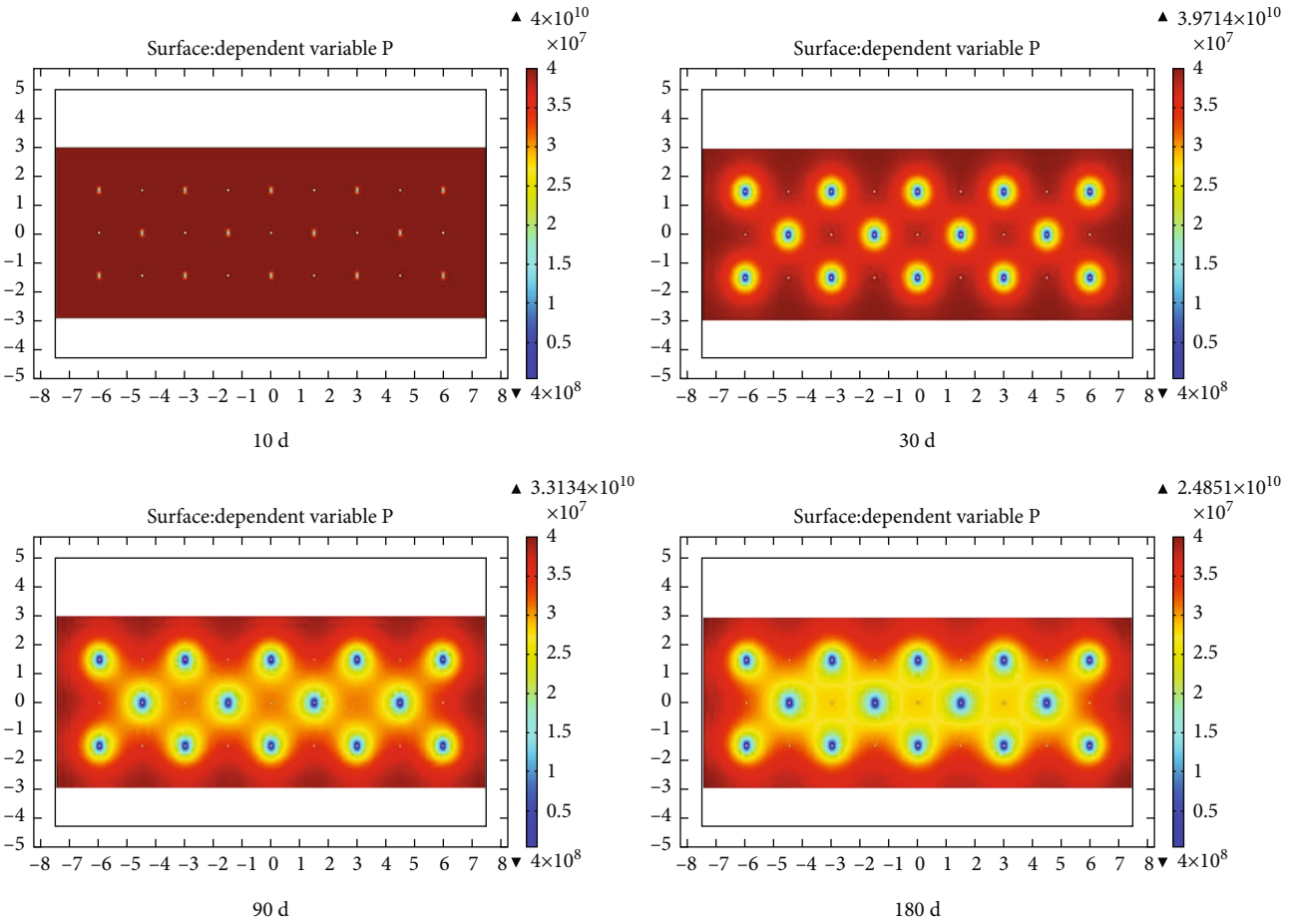

Figure 18: Gas pressure distribution map of mesh hole fracturing.

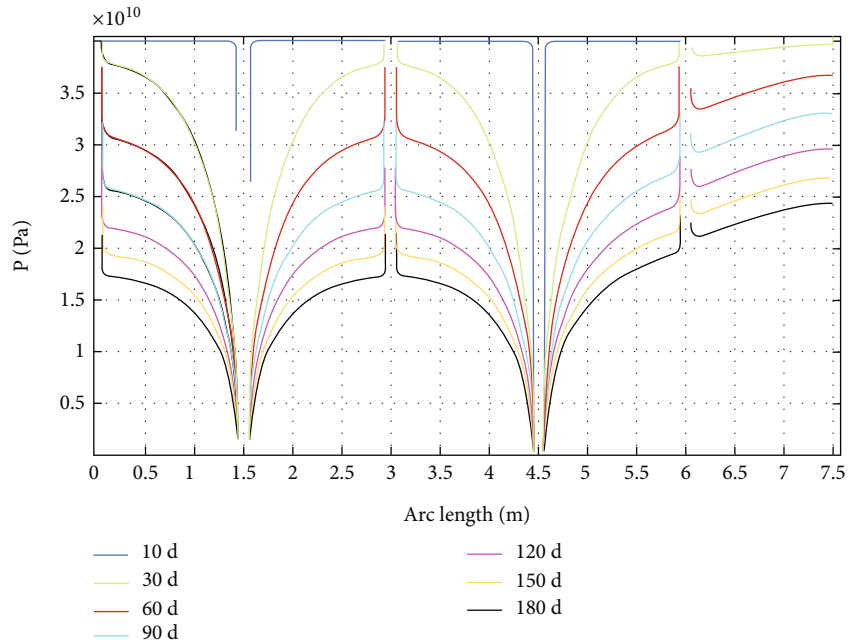

Figure 19: Curves of gas pressure versus distance in mesh fracturing.

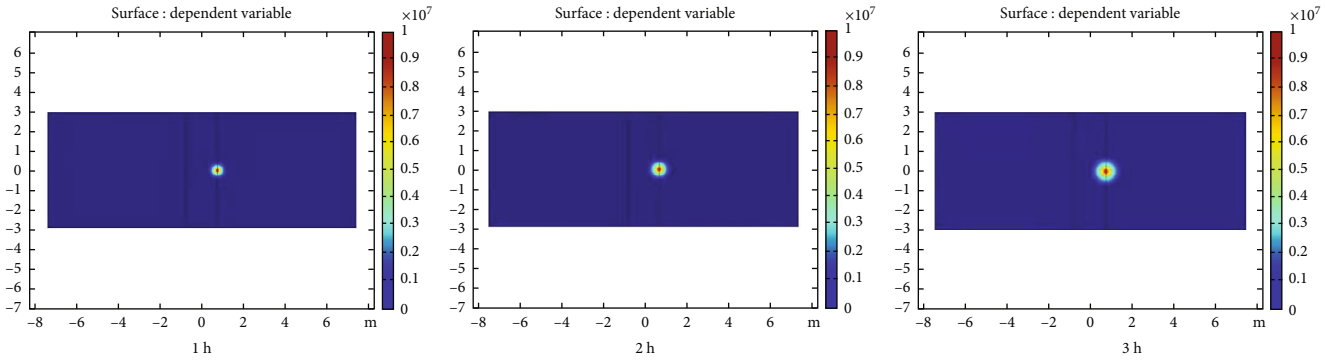

Figure 20: Cloud map of carbon dioxide pressure over time.

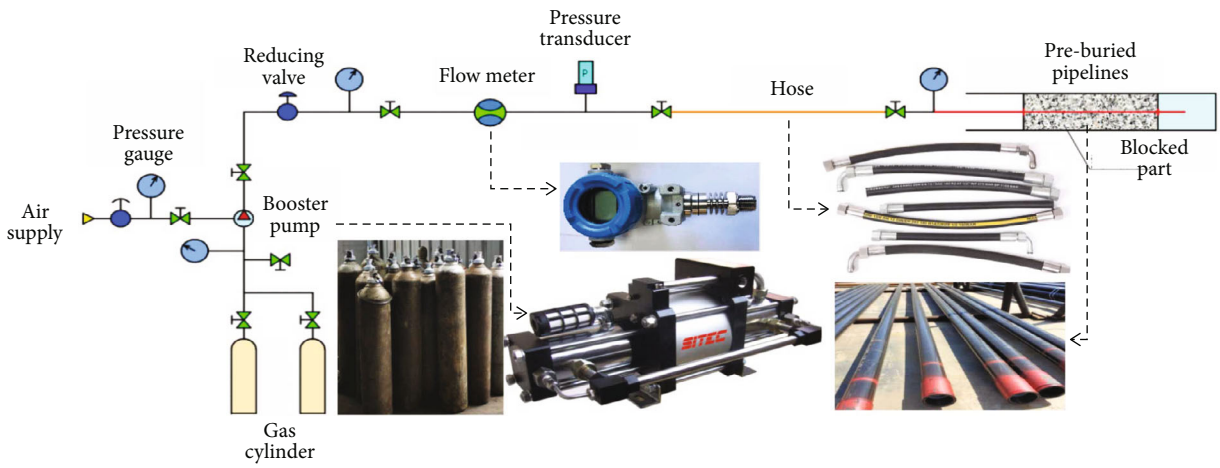

Figure 21: Underground liquid carbon dioxide fracturing antireflection system.

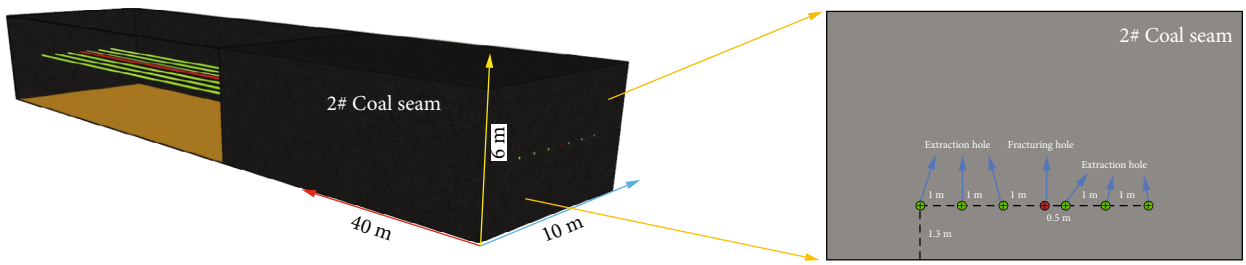

Figure 22: Influence range of carbon dioxide fracturing inspection borehole arrangement.

decompression control valve, flow automatic monitoring system, high pressure armor hose connected to the above device, seamless carbon steel pipe, explosion-proof monitoring and control device, and mine flat car equipped with the above device. In the process of fracturing, the pressure of liquid carbon dioxide storage tank is maintained between 5 MPa and 10 MPa in the process of entering and discharging liquid, which ensures that the continuous transportation of liquid in the pipeline is not easy to plug and can realize high pressure liquid carbon dioxide fracturing of coal seam. The booster pump adopts SITEC brand, GB series gas booster pump, mainly used for carbon dioxide gas pressurization. Model GB 25, pressure ratio 25 : 1, maximum outlet pressure 207.5 Bar, minimum inlet pressure 15 Bar, maximum displacement 114 L/min. The power source of the gas booster pump is the low pressure air source with the maximum output of 0.8 MPa.

6.3. Field Drilling Arrangement Scheme. In order to investigate the influence range of liquid carbon dioxide fracturing and displacement pumping, the fracturing site was selected at 60 m ahead of the 850 m chamber of the return airway in the 12316 fully mechanized mining face of Wangjialing Coal Mine. The fracturing hole was arranged as the inspected hole to the center, and the other inspection holes were arranged to the left and right ends of the fracturing

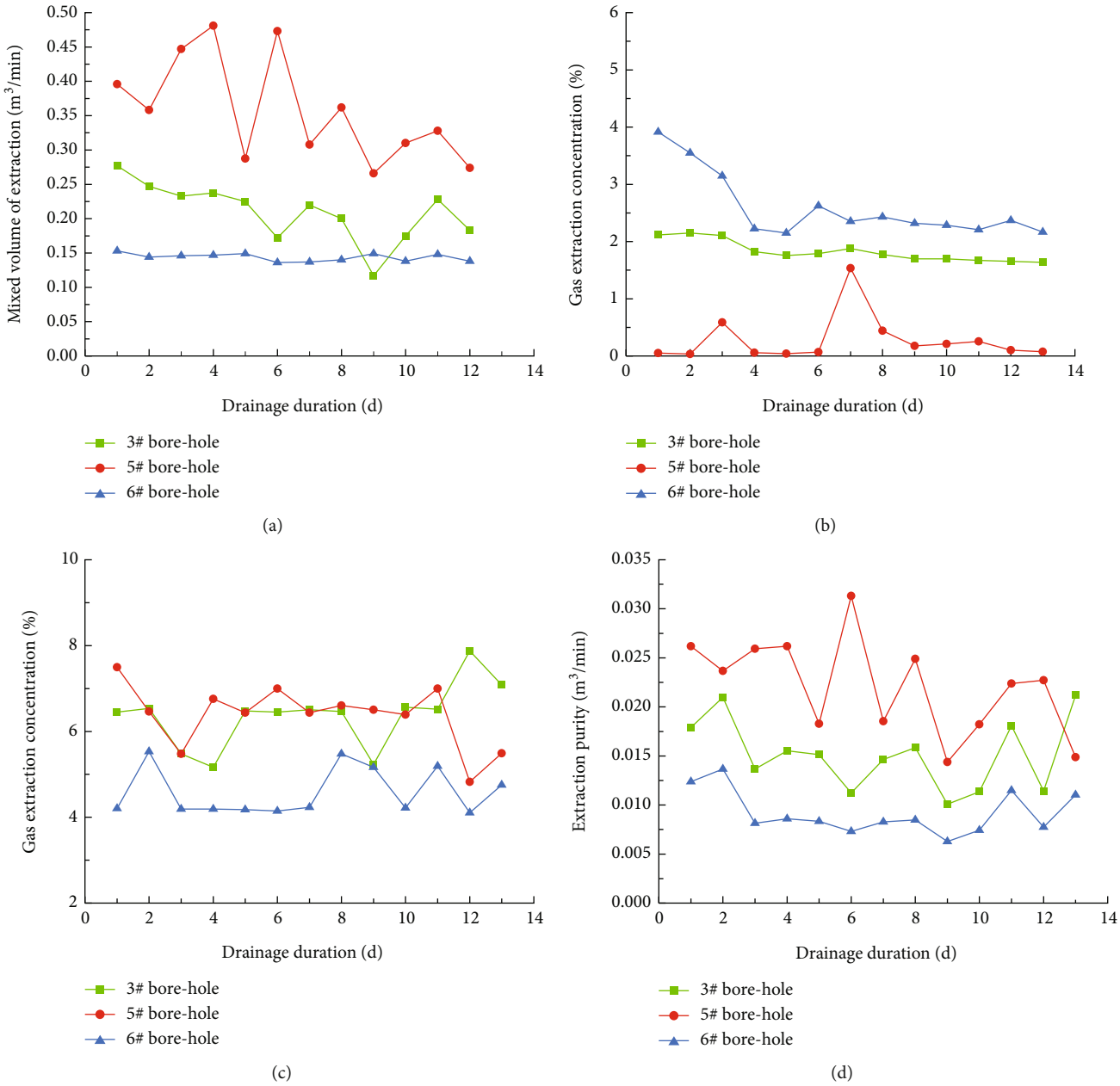

Figure 23: Gas drainage in boreholes 3 #, 5 #, and 6 #.

hole. A total of 7 boreholes were vertical to the coal wall. The borehole diameter was 75 mm, and the hole depth was 40 m. The arrangement of the boreholes in the influence range of fracturing is shown in Figure 22.

6.4. Investigation Results of Extraction Effect. The 4 # fracturing borehole underwent three intermittent liquid carbon dioxide fracturing, and the cumulative injection volume was about 6 m^3. After fracturing, the gas drainage effect and carbon dioxide concentration of 3 #, 5 #, and 6 # inspection holes around the fracturing hole were investigated.

Figure 23(a) shows that after liquid carbon dioxide fracturing, the average extraction mixing amount of 3 #, 5 #, and 6 # boreholes is 0.0791 m^3/min, which is increased to 0.329 m^3/min, 0.204 m^3/min, and 0.143 m^3/min, respectively. This shows that after liquid carbon dioxide fracturing, within the radius of 1.5 m, the flow increase effect appears in the inspection hole, and with the increase of the distance between the inspection hole and the injection hole, the flow increase effect gradually weakens. However, the carbon dioxide concentration shows the opposite trend, as shown in Figure 23(b). This is because boreholes 3 #, 5 #, and 6 # were completed after the injection of borehole 4 #, and the fractures around the observation borehole close to the injection borehole were developed, and the carbon dioxide concentration remaining in the coal seam after fracturing was low. On the contrary, in the extraction borehole far from the injection borehole, the fracture development was small, and the carbon dioxide residue in the coal seam was large (Figure 23(c)). The change of gas drainage concentration

after liquid carbon dioxide injection is consistent with the change of gas drainage concentration after 4 # borehole injection, and the change of gas drainage concentration before and after fracturing is not obvious. Figure 23(d) shows that after liquid carbon dioxide fracturing, the average value of gas extraction purity of boreholes 3 #, 5 #, and 6 # increases from 0.00485 m^3/min to 0.025 m^3/min, 0.018 m^3/min, and 0.011 m^3/min with the increase of the distance from the injection hole, which increases by 5.15 times, 3.71 times, and 2.26 times, respectively. Comparing the gas drainage effect of borehole after liquid carbon dioxide fracturing with that of static fracturing, it is found that liquid carbon dioxide fracturing is more beneficial to the gas drainage of coal seam.

7. Conclusions

(1) The mechanism of liquid carbon dioxide fracturing was analyzed, and the effect of liquid carbon dioxide on coal and gas in coal was expounded from three aspects of "permeability enhancement and displacement-displacement." The feasibility of liquid carbon dioxide fracturing was demonstrated from the side

(2) The mathematical model of fracture expansion is established, and the functional relationship between the pore pressure p_0 of the injection borehole and the fracture expansion radius L is established. The influence of the injection parameters (injection pressure, injection flow rate, and fracturing fluid viscosity) on the fracture expansion radius is emphatically analyzed. When the injection flow rate is constant and the injection pressure difference is constant, the larger the crack width, the larger the corresponding propagation distance, and the influence of crack width on the crack propagation distance is more obvious than that of fracturing fluid viscosity. When the crack width is doubled, the crack propagation distance increases sharply. The fracture toughness K_{IC}, formation pressure σ_1 and σ_3, injection pressure p_0, and fracturing fluid viscosity μ all affect the fracture propagation in coal and rock mass. With the increase of injection pressure difference, the fracture propagation radius increases gradually. When the injection pressure is small, the crack propagation radius is not sensitive to the change of injection pressure difference; when the injection pressure difference is large, the injection pressure has a great influence on the fracture diffusion radius, and the increase of the injection pressure will lead to the obvious change of the fracture diffusion radius

(3) When the injection flow rate is constant, under the condition of the same injection pressure difference, the larger the fracturing fluid viscosity, the smaller the fracture propagation distance; compared with water fracturing and liquid carbon dioxide fracturing, liquid carbon dioxide fracturing has a longer crack propagation distance under the same injection flow and pressure difference due to the low viscosity of liquid carbon dioxide. Due to the low viscosity and strong diffusion of liquid carbon dioxide, there are many cracks produced by fracturing. With the increase of drainage time after fracturing, the gas pressure around the drainage borehole on both sides of the fracturing hole decreases continuously, and the drainage pressure relief range gradually expands and begins to pass. The pressure relief effect of double-hole fracturing is obviously greater than that of single-hole fracturing. In the early stage of extraction, the pressure relief area of the two extraction holes is circular and then gradually evolves into "∞" distribution. The pressure relief effect near the side of the fracturing hole is more obvious

(4) In the control group of fracturing hole spacing 2 m, 3 m, 4 m, and 5 m, the hole spacing of 3 m can achieve good gas drainage effect; compared with single-hole fracturing and double-hole fracturing, the gas drainage effect of mesh hole fracturing is better, and the gas pressure of the whole coal seam is fully released after 180 days

(5) In the same extraction period, the smaller the distance between the extraction hole and the fracturing hole, the larger the gas pressure relief range. The fracture development around the hole near the injection hole is larger, and the carbon dioxide concentration remaining in the coal seam after fracturing is lower. On the contrary, the fracture development is smaller in the extraction hole far from the injection hole, and the carbon dioxide residue in the coal seam is more

Data Availability

The data used to support the findings of this study are included within the article.

Conflicts of Interest

The authors declare that they have no conflicts of interest regarding the publication of this paper.

Acknowledgments

This work is supported by the National Natural Science Foundation of China (Grant Nos. 51904266 and 52104224), Excellent Youth Project of Hunan Provincial Department of Education (Grant No. 21B0144), and Research Project on Teaching Reform of Colleges and Universities in Hunan Province in 2020 (Grant No. HNJG-2020-0231).

References

[1] X. Zhang and J. Zou, "Research on collaborative control technology of coal spontaneous combustion and gas coupling

disaster in goaf based on dynamic isolation," *Fuel*, vol. 321, article 124123, 2022.

[2] Y. Lei, Y. Cheng, L. Wang, T. Ren, and Q. Li, "Potential infrasonic tremors in coal seam systems: implications for the prediction of coal and gas outbursts," *Fuel*, vol. 326, article 125000, 2022.

[3] A. Zhou, M. Zhang, K. Wang, D. Elsworth, J. Wang, and L. Fan, "Airflow disturbance induced by coal mine outburst shock waves: a case study of a gas outburst disaster in China," *International Journal of Rock Mechanics and Mining Sciences.*, vol. 128, article 104262, 2020.

[4] H. Quan, "Influence of coal seam water injection on gas desorptionand release in roadway and its control mechanism," *China Coal*, vol. 47, pp. 30–37, 2021.

[5] C. Hou, B. Jiang, M. Li, Y. Song, and G. Cheng, "Micro-deformation and fracture evolution of in-situ coal affected by temperature, confining pressure, and differential stress," *Journal of Natural Gas Science and Engineering*, vol. 100, article 104455, 2022.

[6] D. Wang, X. Tian, J. Wei et al., "Fracture evolution and nonlinear seepage characteristic of gas-bearing coal using X-ray computed tomography and the lattice Boltzmann method," *Journal of Petroleum Science and Engineering*, vol. 211, article 110144, 2022.

[7] C. Liu, P. Zhang, Y. Ou, D. Yao, and Y. Tian, "Analytical stress analysis method of interbedded coal and rock floor over confined water: a study on mining failure depth," *Journal of Applied Geophysics*, vol. 204, article 104720, 2022.

[8] S. Tang, B. Zhu, and Z. Yan, "Effect of crustal stress on hydraulic fracturing in coalbed methane wells," *Journal of China Coal Society*, vol. 36, pp. 65–69, 2011.

[9] Y. Hu, W. Li, X. Chen, H. Xu, and S. Liu, "Temporal and spatial evolution characteristics of fracture distribution of floor strata in deep coal seam mining," *Engineering Failure Analysis.*, vol. 132, article 105931, 2022.

[10] C. Zhai, X. Li, and Q. Li, "Research and application of pressure relief and permeability enhancement technology of pulsating hydraulic fracturing in coal seam," *Journal of China Coal Society*, vol. 36, pp. 1996–2001, 2011.

[11] H. Xie, F. Gao, H. Zhou, H. Cheng, and F. Zhou, "On theoretical and modeling approach to mining-enhanced permeability for simultaneous exploitation of coal and gas," *Journal of China Coal Society*, vol. 38, pp. 1101–1108, 2013.

[12] Z. Wang, Y. Fan, and S. Li, "Application of borehole hydraulic flushing technology to soft and outburst seam with low permeability," *Coal Science And Technology*, vol. 40, pp. 52–55, 2012.

[13] X. Wang, W. Liu, X. Jiang, Q. Zhang, and Y. Wei, "Evolution characteristics of overburden instability and failure under deep complex mining conditions," *Geofluids*, vol. 2020, Article ID 6418082, 16 pages, 2022.

[14] Z. Huo, "New technology of carbon dioxide fracturer applied to deep borehole pre-cracking blasting for seam permeability improvement," *Coal Science And Technology*, vol. 43, pp. 80–83, 2015.

[15] Y. Shi, B. Lin, T. Liu, Y. Zhao, and Z. Hao, "Synergistic ECBM extraction technology and engineering application based on hydraulic flushing combing gas injection displacement in low permeability coal seams," *Fuel*, vol. 318, article 123688, 2022.

[16] D. Guo, C. Zhang, K. Li, and T. Zhu, "Cracking mechanism of deep hole micro - differential polymerization blasting in soft and low permeability coal seam," *Journal of China Coal Society*, vol. 46, pp. 2583–2592, 2021.

[17] C. Zheng, B. Jiang, L. Yuan et al., "Effects of heterogenous interburden Young's modulus on permeability characteristics of underlying relieved coal seam: Implementation of damage-based permeability model," *Journal of Natural Gas Science and Engineering.*, vol. 96, article 104317, 2021.

[18] R. Feng, "Comparative study on permeability enhancement effect of separate-layer fracturing and multi-layers comprehensive fracturing in coal seam group," *Safety in Coal Mines*, vol. 52, pp. 21–28, 2021.

[19] S. Hazarika and A. Boruah, "Supercritical CO_2 (SCO_2) as alternative to water for shale reservoir fracturing," *Materials Today: Proceedings*, vol. 50, pp. 1754–1757, 2022.

[20] X. Liu, G. Xu, Y. Wang, and Z. Li, "Research and application of permeability enhancement by gas phase fracturing in rapid excavation of coal roadway," *China Energy and Environmental Protection*, vol. 43, pp. 14–18+23, 2021.

[21] Y. Lu, Y. Liao, J. Tang, X. Zhang, S. Han, and Y. Lin, "Experimental study on fracture initiation pressure and morphology in shale using supercritical CO_2 fracturing," *Journal of China Coal Society*, vol. 43, pp. 175–180, 2018.

[22] X. Li, Y. He, M. Huo, Z. Yang, H. Wang, and R. Song, "Model for calculating the temperature and pressure within the fracture during supercritical carbon dioxide fracturing," *International Journal of Hydrogen Energy.*, vol. 45, no. 15, pp. 8369–8384, 2020.

[23] W. Zhu, X. Zhang, S. Liu, C. Wei, J. Wang, and H. Liu, "An experimental apparatus for supercritical CO_2 fracturing of shale: system design and application tests," *Journal of Natural Gas Science and Engineering*, vol. 103, article 104656, 2022.

[24] C. Xu, G. Yang, K. Wang, and Q. Fu, "Uneven stress and permeability variation of mining-disturbed coal seam for targeted CBM drainage: a case study in Baode coal mine, eastern Ordos Basin, China," *China. Fuel*, vol. 289, article 119911, 2021.

[25] H. Zhao, C. Liu, Y. Xiong, H. Zhen, and X. Li, "Experimental research on hydraulic fracture propagation in group of thin coal seams," *Journal of Natural Gas Science and Engineering*, vol. 103, article 104614, 2022.

[26] Z. Shang, H. Wang, B. Li et al., "The effect of leakage characteristics of liquid CO_2 phase transition on fracturing coal seam: applications for enhancing coalbed methane recovery," *Fuel*, vol. 308, article 122044, 2022.

[27] Y. You, "Analysis of well selection and layer selection method of repeated fracturing and influencing factors of fracturing effect," *China Petroleum and Chemical Standard and Quality*, vol. 40, pp. 7-8, 2020.

[28] Z. Zhang, "Analysis of main controlling factors of effective radius of fracture in soft coal seam," *Mining Safety and Environmental Protection*, vol. 4, pp. 99–103+108, 2021.

[29] Q. Hu, Z. Jiang, Q. Li et al., "Induced stress evolution of hydraulic fracturing in an inclined soft coal seam gas reservoir near a fault," *Journal of Natural Gas Science and Engineering*, vol. 88, article 103795, 2021.

[30] A. Lv, L. Cheng, M. A. Aghighi, H. Masoumi, and H. Roshan, "A novel workflow based on physics-informed machine learning to determine the permeability profile of fractured coal seams using downhole geophysical logs," *Marine and Petroleum Geology*, vol. 131, article 105171, 2021.

[31] Z. Lian, J. Zhang, X. Wang, H. Wu, and B. Xue, "Simulation study of characteristics of hydraulic fracturing propagation," *Rock and Soil Mechanics*, vol. 30, pp. 169–174, 2009.

[32] Z. Lian, J. Zhang, X. Wang, H. Wu, and B. Xue, "A simulation study of hydraulic fracturing propagation with a solid-fluid coupling model," *Rock and Soil Mechanics*, vol. 11, pp. 3021–3026, 2008.